SAND2006-7353C

PROBING WATER DYNAMICS IN OCTAHEDRAL MOLECULAR SIEVES: HIGH SPEED ^{1}H MAS NMR INVESTIGATIONS

Todd M. Alam, Jason Pless and Tina M. Nenoff

Sandia National Laboratories, Albuquerque, NM 87185

ABSTRACT

The water dynamics in a series of Sandia octahedral molecular sieves (SOMS) were investigated using high speed ^{1}H magic angle spinning (MAS) NMR spectroscopy. For these materials both the 20% Ti-substituted material, $Na_2Nb_{1.6}Ti_{0.4}(OH)_{0.4}O_{5.6}\bullet H_2O$ and the 0% exchanged end member, $Na_2Nb_2O_6\bullet H_2O$ were studied. By combining direct one dimensional (1D) MAS NMR experiments with double quantum (DQ) filtered MAS NMR experiments different water environments within the materials were identified based on differences in mobility. Two dimensional (2D) DQ correlation experiments were used to extract the DQ spinning sideband patterns allowing the residual ^{1}H-^{1}H homonuclear dipolar coupling to be measured. From these DQ experiments the effective order parameters for the different water environments were calculated. The water environments in the two different SOMS compositions investigated revealed very large differences in the water mobility.

INTRODUCTION

The Sandia octahedral molecular sieves (SOMS) are materials with the general formula $Na_2Nb_{2-x}M^{IV}_xO_{6-x}\bullet H_2O$ (M^{IV} = Ti, Zr) [1, 2]. This class of materials has proven to be extremely efficient ion exchange materials. For example, the 20% Ti exchanged SOMS, $Na_2Nb_{1.6}Ti_{0.4}(OH)_{0.4}O_{5.6}\bullet H_2O$ exhibits selectivity for divalent cations or monovalent cations, with distribution coefficients (Kd) > 99,800 for Sr^{2+} and Ba^{2+} [1]. The impact of heterovalent substitution on the final material properties has been studied, and has shown that increasing Ti stabilizes the resulting SOMS framework, while increasing levels of Zr destabilizes the SOMS framework. In addition, it has been reported that the degree of M^{IV} substitution within the framework changes the divalent cation selectivity within these materials [2]. The selectivity and the stability of these SOMS have been partially related to the presence of framework hydroxyl species and the possibility of hydrogen bonding within the pore structure.

In this paper, the role of water and hydrogen bonding within the pore structure of the SOMS will be further explored; specifically to determine if the dynamics of the waters within the pores are related to the observed selectivity. Water dynamics in materials are commonly investigated using ^{2}H NMR [3-10] which requires the isotopic synthesis or exchange to incorporate D_2O within the material. This process can be time consuming and in some instances difficult. In addition, if the water environments are to be probed following sequential exchange processes with different cations (Sr^{2+}, Ba^{2+} etc), each of the exchange steps must utilize D_2O to retain the ^{2}H isotopic label within the material. To bypass the need for this ^{2}H labeling, we report ^{1}H MAS NMR methods that allow details about the water environments to be determined at natural abundance.

THEORETICAL AND EXPERIMENTAL DETAILS

Synthesis

The synthetic preparation of the octahedral molecular sieves has previously been described in detail [1, 2]. In a typical reaction, niobium(V) ethoxide and titanium tetraisopropoxide were combined in a 4:1 through 20:1 ratio Nb:Ti ratio in a 5 mL vial under an inert atmosphere. The total alkoxide concentration is approximately 10 mmol. The alkoxide mixture is capped and removed from the drybox and treated ultrasonically to ensure thorough mixing. Sodium hydroxide dissolved in deionized water was transferred to a 23 mL Teflon liner for a pressurized Parr® reactor. The alkoxides are quickly added to the NaOH solution, while stirring. The Teflon liner containing the aqueous mixture is placed inside a steel pressure reactor, which is placed in an oven at 443 K for 4 h to 4 days. The resulting product was filtered and washed. The yield for a typical reaction is approximately 1.5 g, or 90% yield based on the initial Ti alkoxide concentration. For the work described here the $Na_2Nb_2O_6 \cdot H_2O$ end member and the 20% Ti SOMS, $Na_2Nb_{1.6}Ti_{0.4}(OH)_{0.4}O_{5.6} \cdot H_2O$ material were studied.

NMR

All solid state ^{1}H MAS NMR spectra were obtained on a Bruker Avance 600 operating at 600.14 MHz, using a 2.5 mm broadband probe at a 30 kHz spinning speed. The ^{1}H chemical shifts were referenced to the solid external secondary sample adamantane (δ = +1.63 ppm with respect to TMS δ = 0.0 ppm). Frictional heating during high speed spinning causes the actual sample temperature to be significantly higher than the regulated temperature. The actual sample temperatures were calibrated using the ^{207}Pb chemical shift change of a secondary $Pb(NO_3)_2$ sample [11, 12], showing a sample temperature of 56 ^{o}C at 30 kHz spinning speed when regulated at 25 ^{o}C. The spin-spin T_2 relaxation times were obtained using a rotor-synchronized Hahn echo. The 1D double quantum filtered (DQF) and the 2D double quantum (DQ) ^{1}H MAS spinning sideband experiments utilized the chemical shift anisotropy (CSA) and off-set compensated back-to-back (BABA) multiple pulse sequence (Figure 1) for the excitation/reconversion of the multiple quantum coherences [13]. For the 2D DQ sideband experiments the $0 \rightarrow \pm 2 \rightarrow 0 \rightarrow 1$ coherence pathway was selected using a 64 step phase cycle, 200-400 non-rotor synchronized t_1 increments, a 3 μs $\pi/2$ pulse length and 8-64 scan averages. The DQF experiments utilized the same sequence, but with a non-incremented 1μs t_1 delay. The 2D DQ sideband patterns were obtained by taking the F_1 slice along the ^{1}H chemical shift of interest, and simulated to determine the effective ^{1}H-^{1}H dipolar coupling.

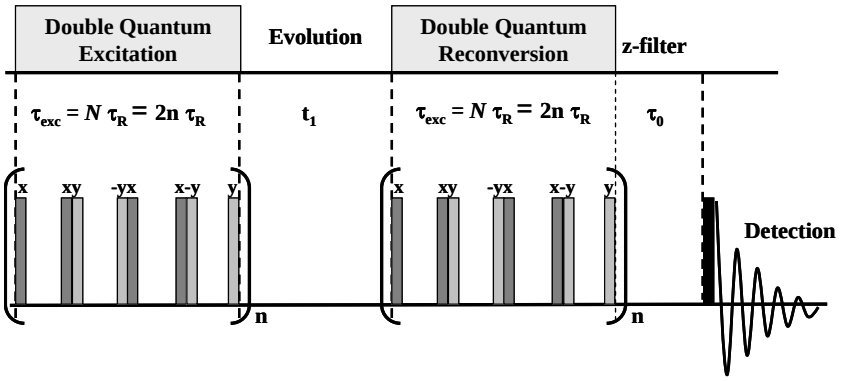

Figure 1: The double quantum (DQ) BABA pulse sequence used for the DQ spinning sideband analysis.

Theory

From the analysis of the 2D double quantum (DQ) ^{1}H MAS NMR experiments it is possible to directly measure the effective ^{1}H-^{1}H dipolar coupling. For a static sample the homonuclear dipolar coupling (D^{ij}) between protons *i* and *j* separated by a distance r_{ij} is given by

$$D_{ij} = \frac{\mu_0 \hbar \gamma_i \gamma_j}{4\pi r_{ij}^3} \tag{1}$$

where μ_0 is the vacuum permeability and $\gamma_{i,j}$ are the magnetic ratios of the interacting protons. Local motions will average these dipolar couplings to produce an effective dipolar coupling. For an isolated spin-1/2 pair (which at first approximation holds for water) with a distribution of couplings, the signal intensity of the DQ sidebands (I_{DQ}) is given by [14]

$$I_{\mathrm{DQ}}(t_1,\rho_l) \sim \sum_l \rho_l \left\langle \sin\left[\frac{3}{\pi\sqrt{2}} D_{\mathrm{eff}}^{ij}(l)\sin\left(2\beta^{ij}\right)\cos\left(\gamma^{ij}+\omega_R t_1\right) N\tau_R\right] \times \sin\left[\frac{3}{\pi\sqrt{2}} D_{\mathrm{eff}}^{ij}(l)\sin\left(2\beta^{ij}\right)\cos\left(\gamma^{ij}\right) N\tau_R\right]\right\rangle \tag{2}$$

where $D_{\mathrm{eff}}^{ij}(l)$ is the *l*th effective dipolar coupling with a probability ρ_l , t_1 is the DQ evolution time increment, $\omega_R\left(=2\pi\nu_R\right)$ is the spinning frequency, *N* is the number of rotor periods in the excitation/reconversion portion of the BABA sequence, $\tau_R\left(=\nu_R^{-1}\right)$ is the rotor period, β^{ij} and γ^{ij} are the Euler angles describing the orientation of the principal axis of the dipolar coupling tensor between spins *i* and *j* within the reference frame fixed to the rotor, and the symbol $\langle\ \rangle$

represents the Euler angle powder average. A Gaussian probability distribution of $D_{\text{eff}}^{ij}(l)$ was assumed with a mean effective dipolar coupling, $\bar{D}_{\text{eff}}^{ij}$, and a standard deviation, σ, defined by

$$\rho_l(\bar{D}_{\text{eff}}^{ij}, \sigma) = \frac{1}{\sqrt{2\pi}} \exp\left[-\frac{1}{2}\left(\frac{\bar{D}_{\text{eff}}^{ij} - D_{\text{eff}}^{ij}(l)}{\sigma} \right)^2 \right] \quad (3)$$

Spectral simulations of the experimental DQ sideband patterns therefore allowed both the mean effective dipolar coupling and the distribution to be measured.

DISCUSSION

The ^{1}H MAS NMR spectrum of the $Na_2Nb_2O_6 \bullet H_2O$ end member SOMS is shown in Figure 2. For this composition the MAS NMR spectra is characterized by a series of spinning sidebands (SSB) even at 30 kHz spinning speed (Figure 2a), consistent with the presence of strong residual ^{1}H-^{1}H homonuclear dipolar coupling. The spectral expansion of the

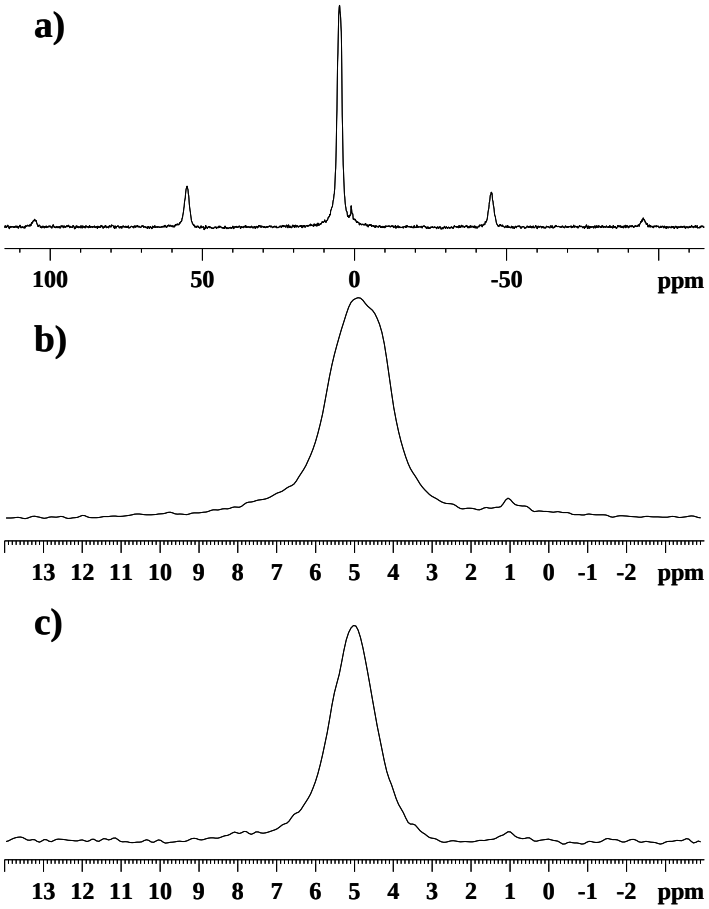

Figure 2: The a) ^{1}H MAS NMR spectrum of $Na_2Nb_2O_6 \bullet H_2O$, b) expansion of the isotropic region and c) the 1D DQ-filtered ^{1}H MAS NMR spectrum.

isotropic resonance region (Figure 2b) reveals three overlapping resonances. To aid in the assignment and resolution of these different ^{1}H species a double quantum filtered (DQF) ^{1}H MAS NMR spectrum was obtained (Figure 2c) using N = 4, 133 μs excitation/reconversion periods. The DQF MAS NMR experiment selects only those protons that have a strong dipolar coupling, such that mobile (including mobile water) or isolated protons are not observed. The DQF ^{1}H NMR spectrum shows a single resonance at δ = +5.0 ppm, with a full width at half-maximum line width (FWHM) of 892 Hz. Using this δ and line width as a constraint the strongly overlapping resonances can be deconvoluted into three distinct spectral components as shown in Figure 3. There is a major ^{1}H resonance at δ = +5.0 ppm (89% relative concentration), a second resonance at δ = +4.3 ppm, FWHM =378 Hz (9%) and a minor species at δ = +1.0 ppm, FWHM 300 Hz (2%). This deconvolution is also consistent with close inspection of Figure 2a, which shows that the line shape for the spinning sidebands are single Lorentzian and are not composed of multiple overlapping resonances as observed in the spectral expansion of the isotropic region. The major ϕ = +5.0 ppm resonance has a T_2 ~ 627 μs. The δ = +5.0 ppm resonance has been assigned to relatively immobile water adsorbed within the molecular sieve. This assignment is supported by the strong DQ signal, and the presence of SSB. The δ = +4.3 ppm resonance is assigned to mobile water species present within the pore or surface of the SOMS. This water species must be mobile enough to effectively average the ^{1}H-^{1}H dipolar coupling to near zero such that neither significant DQ signal nor SSB are observed. The final resonance at δ = +1.0 ppm is assigned to a NbOH species as discussed in previous studies of SOMS [2] and other related polyoxoniobates [15].

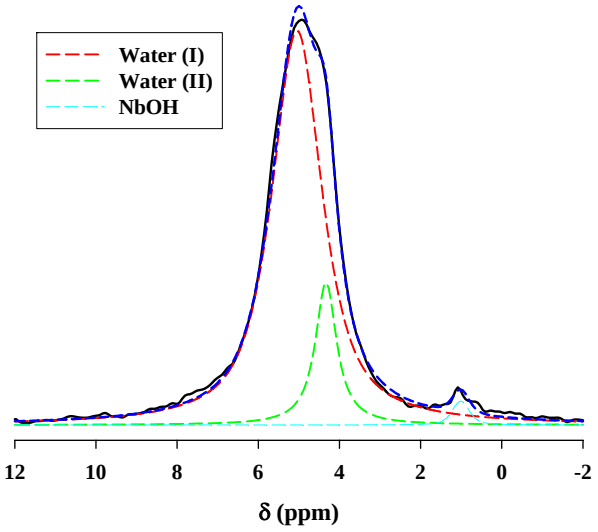

Figure 3: The ^{1}H MAS NMR spectral deconvolution of the central isotropic resonance in $Na_2Nb_2O_6•H_2O$.

The ^{1}H MAS NMR spectrum of the 20% Ti SOMS, $Na_2Nb_{1.6}Ti_{0.4}(OH)_{0.4}O_{5.6}•H_2O$, is shown in Figure 4. Unlike the $Na_2Nb_2O_6•H_2O$ end member SOMS material, no significant SSBs were observed at 30 kHz spinning speed (Figure 4a). Only a single resonance at δ = +4.7 ppm, FWHM = 447 Hz is resolved. This resonance shows bi-exponential T_2 decay, with a small T_2 ~

430 µs decaying fraction and a major T_2 ~1610 µs decaying component. The 1D DQF MAS NMR spectrum (Figure 4c) shows a weak resonance at δ = +4.8 ppm (FWHM 742 Hz). This filtered component accounts for less than 5% of the total ^{1}H signal. A well constrained deconvolution of the 1D MAS NMR spectrum (Figure 4b) into multiple overlapping resonances was not possible. The resonance at δ = +4.7 ppm is assigned to mobile waters in the 20% Ti SOMS which is consistent with the lack of significant DQ signal, SSB and a ~ 50% reduction in line width compared to the $Na_2Nb_2O_6 \bullet H_2O$ material.

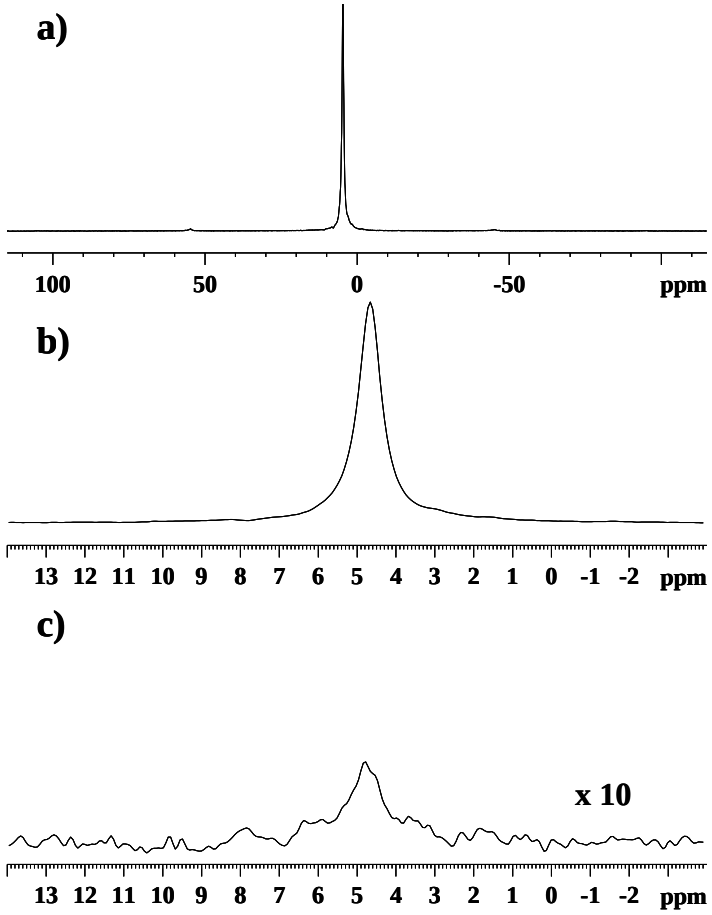

Figure 4: The a) ^{1}H MAS NMR spectrum of $Na_2Nb_{1.6}Ti_{0.4}(OH)_{0.4}O_{5.6} \bullet H_2O$, b) expansion of the isotropic region and c) the 1D DQ-filtered ^{1}H MAS NMR spectrum.

The discussion of the different water environments to this point has been qualitative in nature, with only the relative water mobilities being compared. It is possible to provide a more quantitative analysis of the water dynamics by simulation of the DQ ^{1}H MAS NMR spinning sideband patterns extracted from the 2D DQ correlation experiment. The response of the DQ spinning sideband patters (Eqn 2) to variations in the ^{1}H-^{1}H dipolar coupling are very distinct and allows the effective dipolar coupling (D_{eff}) to be determined [14]. The ^{1}H DQ MAS NMR sideband pattern for the $Na_2Nb_2O_6 \bullet H_2O$ SOMS is shown in Figure 5, along with the spectra simulation. In Figure 5 odd-ordered sidebands from ±1 to ±17 are visible. The even ordered side bands are known to arise from multi-spin interactions [14]. The presence of these higher order

odd spinning sidebands immediately shows that the water species in this SOMS material have a very large residual dipolar coupling. This means the local water dynamics are limited and do not significantly average this interaction. From spectral simulations values of D_{eff} = 28 kHz, with σ = 4 kHz were obtained for $Na_2Nb_2O_6 \bullet H_2O$.

Using this effective dipolar coupling it is possible to then calculate a water order parameter (S_{H_2O}) defined by

$$S_{H_2O} = \bar{D}^{ij}_{\text{eff}} / D^{ij}_{\text{rigid}} \qquad (4)$$

where D^{ij}_{rigid} is the dipolar coupling in a motionally rigid water molecule, and S_{H_2O} can range between 0 and 1. For a water molecule with a ^1H-^1H distance of 1.54 Å, a dipolar coupling ($D^{ij}_{\text{rigid}} / 2\pi$) of 33.4 kHz is predicted using Eqn 1 [16]. Using this relationship, S_{H_2O} ~0.84 for $Na_2Nb_2O_6 \bullet H_2O$. The large S_{H_2O} value experimentally observed limits the type of water dynamics

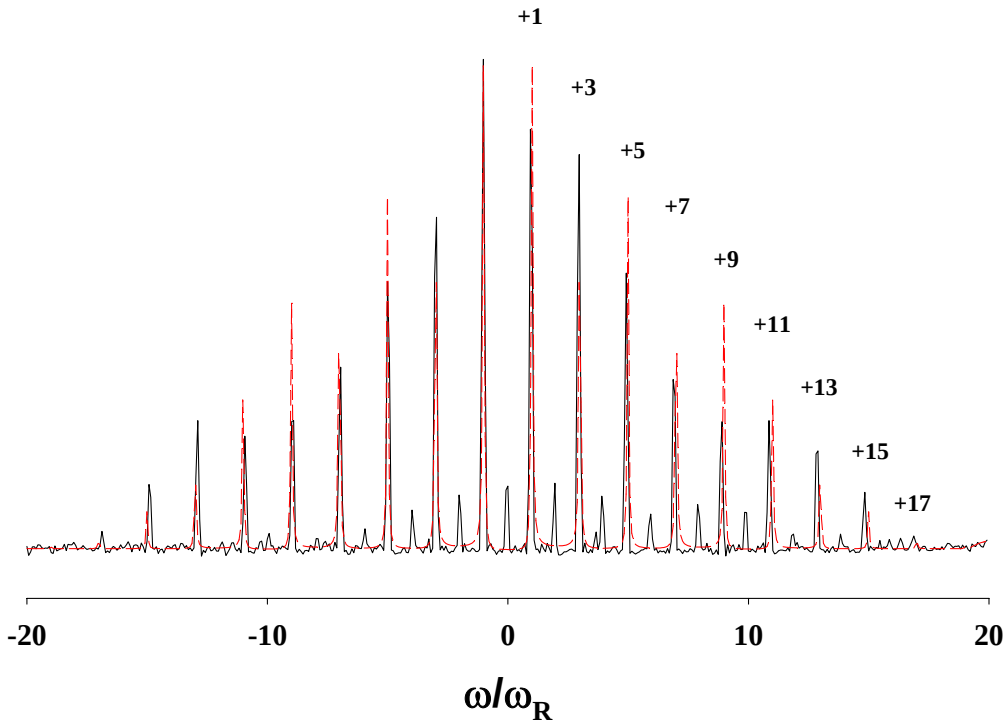

Figure 5: The DQ spinning sideband pattern spectrum (black) and simulated spectrum (red) for $Na_2Nb_2O_6 \bullet H_2O$.

that can be occurring within the pores of this SOMS material. There have been numerous motional models used to describe water dynamics in materials [17-20]. The presence of discrete 180° jumps about the C_{2V} symmetry axis of the H_2O molecule will not produce an averaging of the ^1H-^1H dipolar coupling, since this motion results in a coincident dipolar tensor. This is in contrast to ^2H NMR where the effective ^2H quadrupolar coupling is averaged by a discrete 2-site

jump because the principal component of the quadrupolar electrical field gradient tensor is aligned approximately along the OD bond axis which changes orientation during the 2-site jump process [10]. On the other hand a continuous spinning motion about the water C_{2V} axis (axis perpendicular to the ^{1}H-^{1}H dipolar tensor axis) averages the ^{1}H-^{1}H dipolar coupling by 1/2 (S_{H_2O} = 0.5) to give a $\bar{D}^{ij}_{\text{eff}}$ of ~ 16.7 kHz. These DQ ^{1}H MAS NMR measurements demonstrates that the majority of water environments in the end member $Na_2Nb_2O_6 \bullet H_2O$ SOMS material have a large motional order parameter, with the small reduction in the order parameters arising from librational type motions. There are no continuous spinning motions around the water C_{2V} axis, while discrete 2-site 180^o jumps around the C_{2V} axis can not be resolved using the present ^{1}H-^{1}H dipolar experiment.

For the 20% Ti SOMS material, $Na_2Nb_{1.6}Ti_{0.4}(OH)_{0.4}O_{5.6} \bullet H_2O$, the majority of the water environments in the material are so mobile that the effective dipolar coupling is vanishingly small. This means that the DQ BABA sequence does not provide sufficient intensity buildup during the excitation/reconversion sequence (i.e. no dipolar coupling, no signal). From previous investigations [14] it is known that for the experimental conditions utilized in this DQ study, this lack of signal limits D_{eff} << 5 kHz. There is a small fraction of water species that is visible in the DQF ^{1}H MAS NMR spectrum (Figure 4c), and corresponds to immobile water species. This limited population of waters species within the pores 20% Ti substituted SOMS also gives rise to a set of DQ spinning sideband patterns similar to those seen in Figure 5, with a $\bar{D}^{ij}_{\text{eff}}$ ~ 28 kHz. This result shows that while the majority of the water species in the 20% Ti SOMS are very mobile, there is a small subpopulation with dynamics that are very similar to the $Na_2Nb_2O_6 \bullet H_2O$ material.

CONCLUSIONS

These high speed ^{1}H MAS NMR investigations demonstrate that the water dynamics in the $Na_2Nb_2O_6 \bullet H_2O$ and the $Na_2Nb_{1.6}Ti_{0.4}(OH)_{0.4}O_{5.6} \bullet H_2O$ SOMS materials are very different. The water in the 20% Ti substituted SOMS has high mobility suggesting that the interactions between the pore surfaces and the channel waters are limited. This is in contrast to the $Na_2Nb_2O_6 \bullet H_2O$ where the waters are immobile, suggesting strong interactions with the pore surface. This difference may be accounted for by the presence of additional OH species incorporated into the structure for charge balance with increasing M^{IV} substitution [1, 2]. This dynamical difference may also be related to subtle changes in the Na hydration sphere and the networking with surrounding waters within the pore [2]. By utilizing 2D DQ ^{1}H MAS NMR experiments it was possible to extract an effective dipolar coupling for the immobile water species in these materials which were found to give an order parameter of ~0.84. These experiments demonstrated that information about the water dynamics could be measured without the need for ^{2}H isotopic synthesis or water exchange. The relationship between the water mobility and the rate of cation exchange and the high selectivity in SOMS will be explored by future studies of multiple compositions. In addition, investigations into the observed water dynamics following exchange of the Na^+ with Sr^{2+} or other cations are in progress.

ACKNOWLEDGMENTS

Sandia is a multiprogram laboratory operated by Sandia Corporation, a Lockheed Martin Company, for the United States Department of Energy's National Nuclear Security Administration under Contract DE-AC04-94AL85000. The work described here was supported under Sandia LDRD program.

REFERENCES

[1]. M. Nyman; A. Tripathi; J. B. Parise; R. S. Maxwell; W. T. A. Harrison; T. M. Nenoff, *J. Am. Chem. Soc.* **123**, 1529 (2001).
[2]. M. Nyman; A. Tripathi; J. B. Parise; R. S. Maxwell; T. M. Nenoff, *J. Am. Chem. Soc.* **124**, 1704 (2002).
[3]. D. Goldfarb; H.-X. Li; M. E. Davis, *J. Am. Chem. Soc.* **114**, 3690 (1992).
[4]. M. Duer; H. He; W. Kolodziejski; J. Klinowski, *J. Phys. Chem.* **98**, 1198 (1994).
[5]. S. Di Benedetto; G. Chidichimo; A. Golemme; D. Imbardelli, *J. Phys. Chem.* **100**, 8079 (1996).
[6]. G. Chidichimo; A. Golemme; D. Imbardelli; E. Santoro, *J. Phys. Chem.* **94**, 6826 (1990).
[7]. A. G. Stepanov; T. O. Shegai; M. V. Luzgin; N. Essayem; H. Jobic, *J. Phys. Chem.* **107**, 12438 (2003).
[8]. M. Mizuno; Y. Hamada; T. Kitahara; M. Suhara, *J. Phys. Chem. A* **103**, 4981 (1999).
[9]. A. Wingen; W. Basler; H. Lechert, Anisotropic Motion of Water in Zeolites EMT, L, and ZSM-5 as Studied by D- and H-NMR Line Splitting. In *Progress in Zeolite and Microporous Materials*, Chon, H.; Ihm, S.-K.; Uh, Y. S., Eds. Elsevier Science B. V.: 1997; Vol. 105, pp 495.
[10]. J. M. Kobe; T. J. Gluszak; J. A. Dumesic; T. W. Root, *J. Phys. Chem.* **99**, 5485 (1995).
[11]. A. Bielecki; D. P. Burum, *Journal of Magnetic Resonance, Series A* **116**, 215 (1995).
[12]. T. Takahashi; H. Kawashima; H. Sugisawa; T. Baba, *Solid State Nuclear Magnetic Resonance* **15**, 119 (1999).
[13]. I. Schnell; H. W. Spiess, *J. Mag. Res.* **151**, 153 (2001).
[14]. G. P. Holland; B. R. Cherry; T. M. Alam, *J. Magn. Reson.* **167**, 161 (2004).
[15]. T. M. Alam; M. Nyman; B. R. Cherry; J. M. Segall; L. E. Lybarger, *J. Am. Chem. Soc.* **126**, 5610 (2004).
[16]. A. Abragam, *Principles of Nuclear Magnetism*. Clarendon Press: Oxford, 1961; p 599.
[17]. P. Batamack; C. Dorémieux-Morin; R. Vincent; J. Fraissard, *Chem. Phys. Lett.* **180**, 545 (1991).
[18]. P. Batamack; C. Dorémieux-Morin; R. Vincent; J. Fraissard, *J. Phys. Chem.* **97**, 9779 (1993).
[19]. T. Udea; N. Nakamura, *J. Phys. Chem. B* **107**, 13681 (2003).
[20]. J. Tritt-Goc; N. Pislewski, *Molecular Physics* **83**, 949 (1994).